UDC 621.45.05.225

F. FORGHANY[1], M. TAIEBI-RAHNI[2], A. ASDOLLAHI-GHOHIEH[3]

[1] ***Science and Research Branch, Islamic Azad University, Tehran, Iran***
[2] ***Sharif University of Technology, Tehran, Iran***
[3] ***Civil Aviation Technology College, Tehran, Iran***

NUMERICAL STUDY OF THE AERODYNAMIC EFFECTS ON FLUIDIC THRUST VECTORING

A computational investigation of the aerodynamic effects on fluidic thrust vectoring was conducted. Simulations of a two-dimensional convergent-divergent (2DCD) nozzle with shock-vector control method of fluidic injection for pitch vector control was performed with CFD, using Spalart-Allmaras (S-A) one equation turbulence model. A static freestream condition (M=0.05) at Mach numbers from M=0.3 to 1.2, with nozzle pressure ratios of 4.6 and secondary to primary total pressure ratios of 0.7 were assumed. The aerodynamic penalty to thrust vector angle ranged from 3.9 degrees with M=1.2 freestream condition to 1.08 degrees with M=0.3 freestream condition, (compared to the same nozzle pressure ratios with static freestream conditions). Results indicate that the freestream flow decreases vectoring performance and thrust efficiency, compared to static (wind-off) condition.

Key words: *thrust vectoring, shock vector control, external freestream mach number effect.*

Introduction

A desirable goal of a jet fighter aircraft designer is to increase the aircraft's maneuverability, survivability, and agility. Fluidic thrust vectoring offers the potential for structurally fixed nozzles, which have the potential for substantial weight reductions (compared to mechanical thrust vectoring nozzles that require actuated hardware to force the exhaust flow off axis).

Fluidic thrust vectoring is the control of the primary exhaust flow with the use of a secondary air source, which typically bleeds air from the engine compressor or fan. Three primary mechanisms of fluidic thrust vectoring are shock-vector control, throat shifting, and counterflow.

These techniques can be used to vector the exhaust flow in the pitch and yaw directions. All thrust vectoring techniques are evaluated with some common parameters. Thrust vector angle and thrust vectoring efficiency. Thrust vectoring efficiency (η) is an important parameter to evaluate and compare the ability of different configurations to vector the primary exhaust flow with a given amount of secondary fluidic injection [1-14].

The shock-vector control (SVC) method [2-9] uses supersonic flow turning through shocks created by fluidic injection in the divergent section of a convergent-divergent (CD) nozzle. Working best at off-design, over-expanded flow conditions, large thrust vector angles are generated with SVC techniques in expense of system thrust ratio, as the flow is robustly turned and losses occur through shocks in the nozzle.

The current investigation attempted to initiate a database of secondary flow injection angle effects on fluidic thrust vectoring. The nozzle under investigation was a two-dimensional, convergent-divergent (2DCD) rectangular nozzle with fluidic injection for pitch thrust vector control. The secondary air stream was injected through a slot in the upper divergent wall. Simulations were computed with nozzle pressure ratio (NPR) of 4.6, secondary pressure ratios (SPR) of 0.7 were also investigated with static freestream condition M∞=0.05 and Mach number from 0.3 to 1.2 to document the effect of the external freestream on vectoring effectiveness and thrust vectoring efficiency, which corresponded to secondary mass flow rates 4% of the primary mass flow rate, respectively [15-17]. In addition, a comparison between computational and experimental results [15] is made to validate computational method as a viable tool for predicting nozzle flows with injection streams.

1. Computational Method

The CFD code PMB3D (Parallel Multi-Block, three-dimensional) was developed and used to predict thrust vectoring efficiency, internal nozzle performance, and fluidic thrust vectoring by convergent-divergent rectangular nozzle concept. PMB3D requires a structured-mesh computational domain and a multi-block feature to allow the domain to be partitioned into different sections, which is critical for

modeling complex configurations (like the 2DCD and for efficiently, running the parallel version). Our Explicit, finite-volume flow solver represents the three-dimensional (3D), unsteady Reynolds-averaged Navier-Stokes (URANS) equations. The URANS equations were solved together with the Spalart-Allmaras (S-A) one equation turbulence model for closure of the URANS equations. AUSM+ flux splitting scheme and 4^{th} order Runge-Kutta scheme for time integration were all implemented in each block. MUSCL interpolation was used to provide high order accuracy with the Van Albada limiter to prevent spurious oscillations across shock waves [18-25].

A first order extrapolation outflow condition was used at downstream far field boundary. The stagnation conditions were specified in nozzle inlet and the injection port with total pressure boundary condition and a fixed total temperature. A no-slip adiabatic wall boundary conditions was implemented on nozzle surfaces to obtain viscous solutions.

The nozzle used in this study was an axisymmetric, rectangular, two-dimensional CD nozzle from NASA Langley Research Center [15]. The length of the nozzle was 115.57 mm, while the nozzle width was 101.346 mm. In addition, the throat area of the nozzle was 2785.19 mm², half height of the throat was 13.741 mm, and 57.785 mm from throat to inlet. The area ratio of the nozzle outlet to the throat (expansion ratio) was 1.796 and nozzle divergence angle was 11.01°. The nozzle inlet center was set to be the origin of coordinates, the secondary inlet located at 104.14 mm and the length of slot was 2.032 mm (Fig's. 1-2).

The computational mesh was three-dimensional with 8 blocks defining the internal nozzle, 1 block representing the injection plenum, and 10 blocks representing the external freestream domain. The injection plenum (Fig. 3) had one-to-one grid matching with the nozzle divergent section mesh. The far field was located 2 nozzle lengths upstream and 8 nozzle lengths downstream of the nozzle exit. The upper and lower lateral far field was located 6 body lengths above and below the nozzle. The first grid height in the boundary layer was defined for $y+<1.5$ on the fine mesh spacing for adequate modeling of the boundary layer flow and its interaction with secondary flow injection.

2. Results

A computational investigation of the aerodynamic effects on fluidic thrust vectoring has been conducted. Simulation of a two-dimensional, convergent-divergent (2DCD) nozzle with shock-vector control method of fluidic injection for pitch vector control were performed using URANS approach and Spalart-Allmaras one equation turbulence model. Simulations were conducted for nozzle pressure ratio (NPR) of 4.6 and secondary pressure ratios (SPR) of 0.7 at $M\infty=0.05$ and free stream Mach number from 0.3 to 1.2; which corresponded to secondary mass flow rates of 4% of the primary mass flow rate. The effect of the external freestrean Mach number on pitch thrust vector angle and thrust vectoring efficiency were investigated. The performance of fluidic thrust vectoring (FTV) was evaluated by thrust vector angle and thrust vectoring efficiency in nozzle exit. The effect of fluidic thrust vectoring parameters, such as the NPR, SPR, and $M\infty$ on FTV performance was studied.

2.1. Code Validation

Our computational results were compared with experimental data of Ref. [15]. The centerline pressure at, SPR=0.7 (4% of primary mass flow rate) is shown in Fig. 1. Our PMB3D results for pitch thrust vector angle and static pressures along the upper and lower nozzle surfaces correlated well with experimental data (with a few correlate well with experimental data (with a few notable exceptional points near shock). The shock location, at the upper surface was predicted to be $x/x_t=1.56$ (x_t is axial location of throat), while it was 1.53 in the experiment. Our results at the lower surface gave $x/x_t=1.91$, compared to 1.89 found by the above experimental (Fig. 4).

2.2. Effect of Freestream Mach Number ($M\infty$)

The thrust vector angle in variable freestream Mach number, which achieved from 10.32° to 6.42° by the optimize fluidic injection angle (110°) is decreased (10.5% to 37.7%). Also from 7.57° to 4.33° by the normal to boundary fluidic injection angle (78.99°) is decreased (16.37% to 42.64%).

The thrust vectoring efficiency is achieved from 3.099°/%- injection to 1.933°/%-injection by the optimize fluidic injection angle is decreased (10.5% to 37.6%). Also from 2.151°/%- injection to 1.107°/%-injection by the normal to boundary fluidic injection angle is decreased (24.73% to 48.53%).

On the other hand increasing freestream Mach number, decreases pitch thrust vector angle in all cases. In addition, it decreases thrust vectoring efficiency in most cases. Mach number shadowgraph and pressure distributions along the nozzle centerline for NPR=4.6 and variable freestream Mach number, (Fig's. 5-6).

Also the effect of increasing freestream Mach number has negative impact on thrust vector angle and thrust vectoring efficiency, (Fig. 7).

Table 1

Effect of freestream Mach number on internal performance decline

Case 1		Fluidic injection angle (normal to boundary)						Decline	
NPR	SPR	M∞	δ_p (deg)	η (deg/%inj)	M∞	δ_p (deg)	η (deg/%inj)	δ_p %	η %
4.6	0.7	0.05	7.578	2.151	0.3	6.337	1.619	16.37	24.73
					0.6	5.84	1.506	22.93	29.98
					0.9	4.119	1.052	45.64	51.09
					1.2	4.332	1.107	42.64	48.53

Case 1		Optimize injection angle (φ= 110°)						Decline	
NPR	SPR	M∞	δ_p (deg)	η (deg/%inj)	M∞	δ_p (deg)	η (deg/%inj)	δ_p %	η %
4.6	0.7	0.05	10.329	3.099	0.3	9.242	2.773	10.5	10.5
					0.6	8.129	2.438	21.3	21.3
					0.9	6.192	1.858	40.1	40
					1.2	6.426	1.933	37.7	37.6

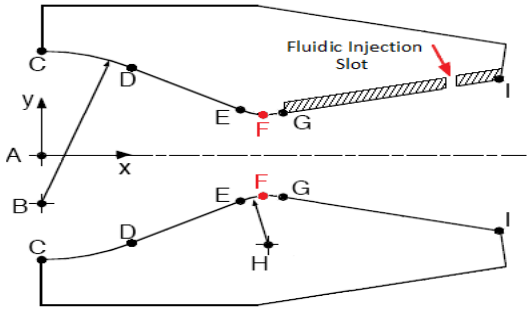

Point	Coordinat	
	X, mm	Y, mm
A	0	0
B	0	-15.595
C	0	35.204
D	23.291	29.541
E	50.495	15.519
F	57.785	13.741
G	60.807	14.046
H	57.785	29.616
I	115.57	24.688

All positions measured from centerline of nozzle

Fig. 1. Sketch of the geometric design for 2DCD rectangular fluidic thrust vectoring nozzle (x-y plane)

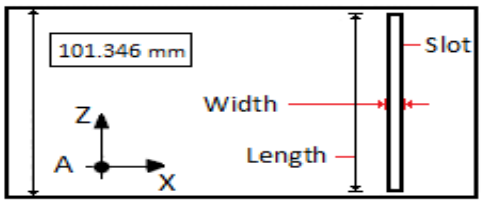

X, mm	Length, mm	Width, mm
104.14	88.646	2.032

Fig. 2. Sketch of the design injection slot for 2DCD rectangular fluidic thrust vectoring nozzle (x-z plane)

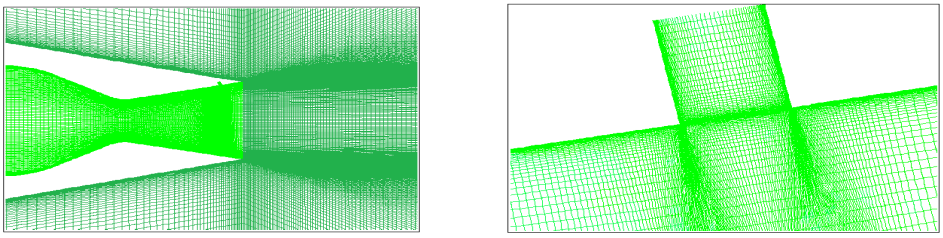

Fig. 3. The computational domain representing the 2DCD nozzle with a injection plenum (the injecton plenum has one-to-one grid matching with the primary nozzle grid)

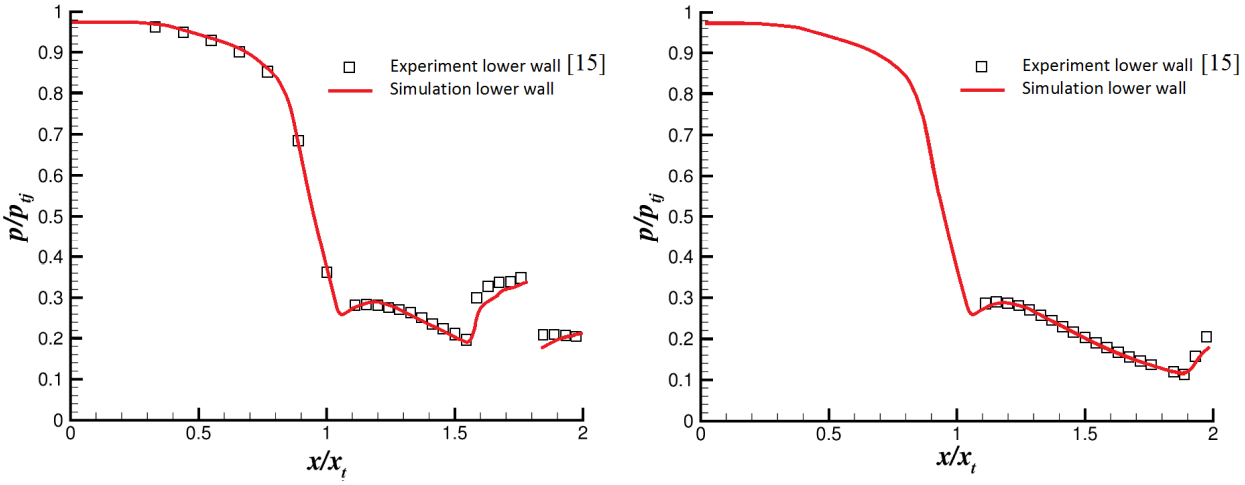

Fig. 4. Experimental and comptational centerline pressure along internal nozzle walls, NPR=4.6, SPR=0.7 at static freestream conditions

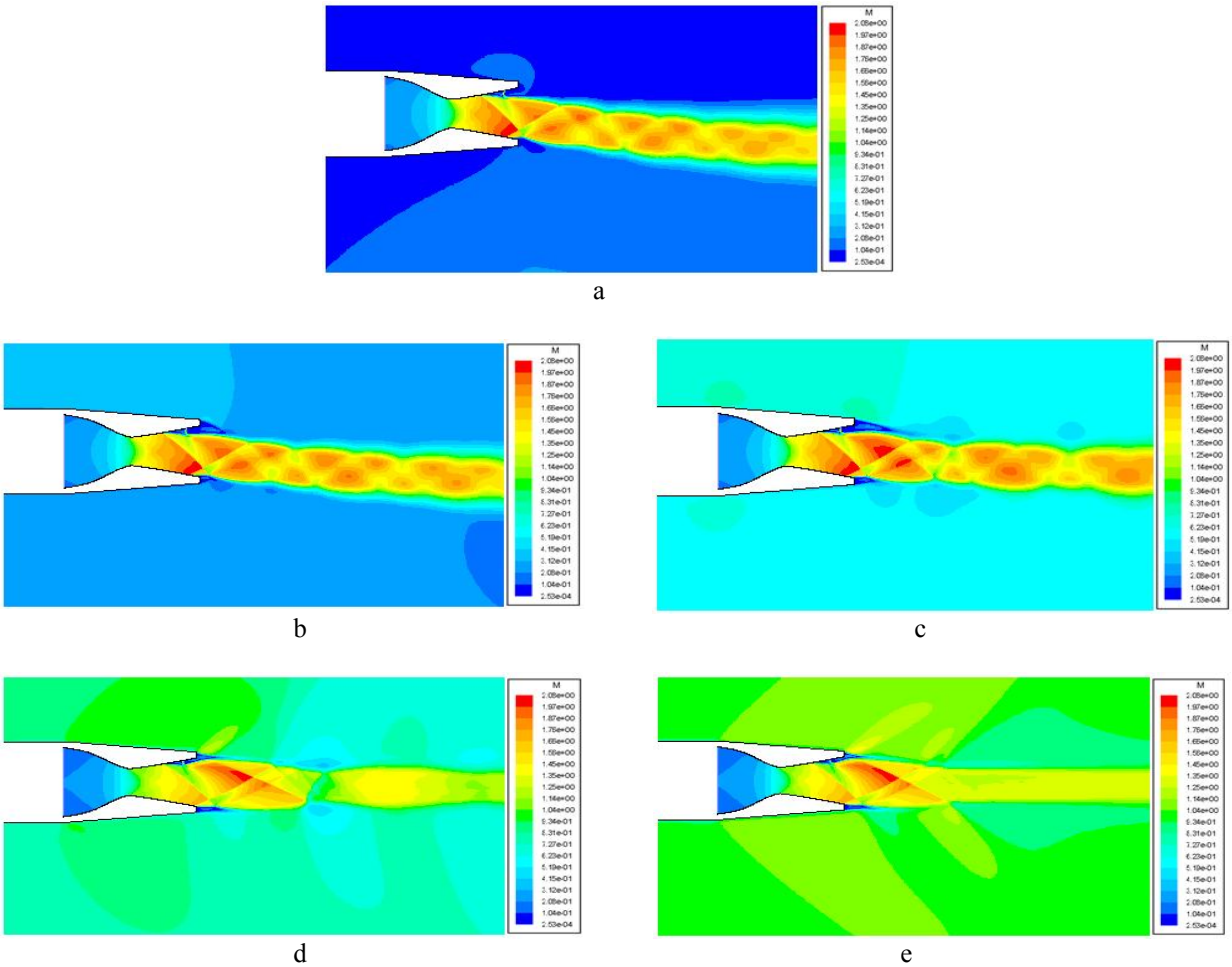

Fig. 5. Mach number shaowgraph inside and outside the nozzle at NPR=4.6 and SPR=0.7 for: (a) M∞=0.05, (b) M∞=0.3, (c) M∞=0.6, (d) M∞=0.9, and (e) M∞=1.2

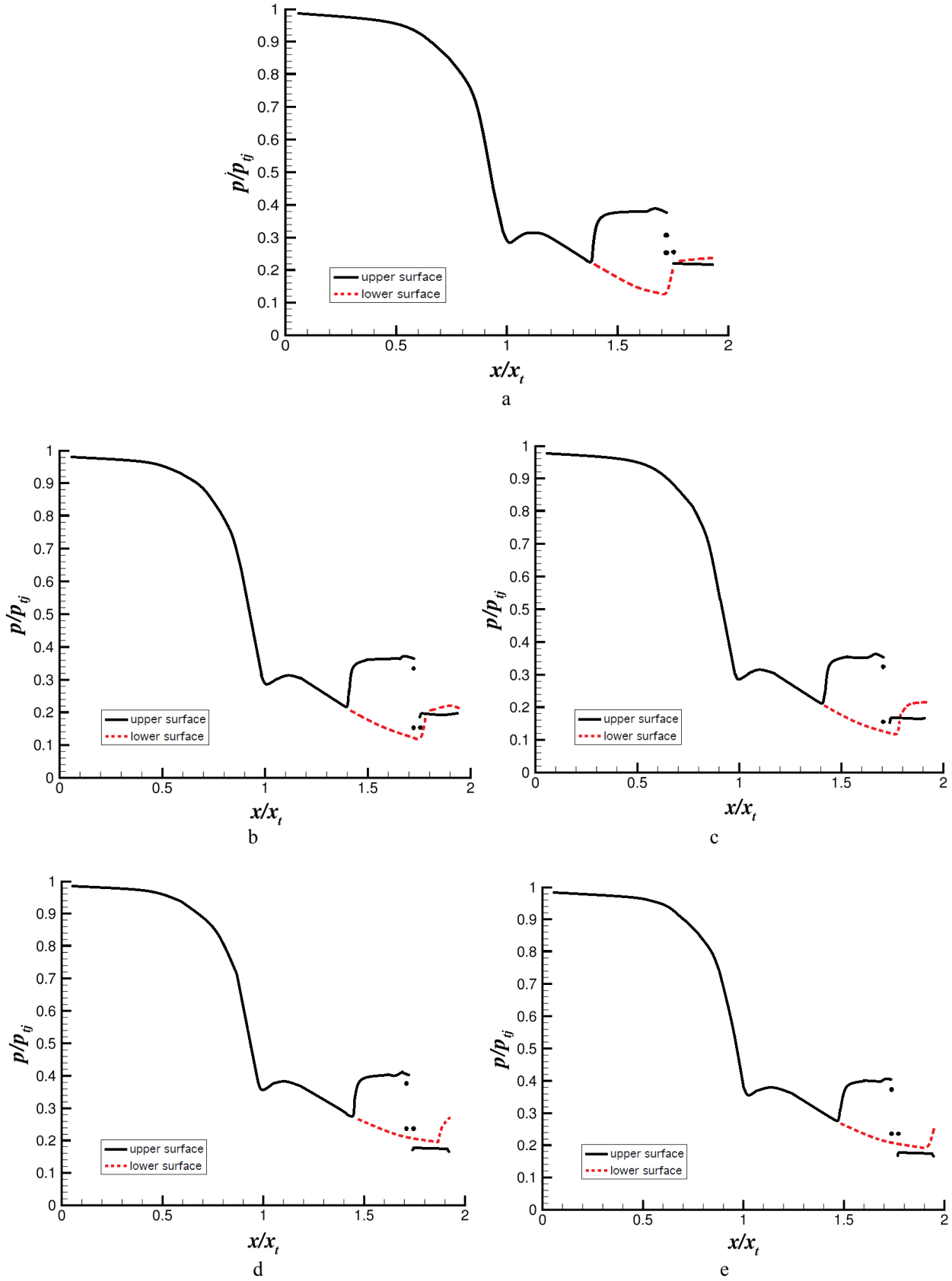

Fig. 6. Pressure distribution along the nozzle centerline at NPR=4.6 and SPR=0.7 for: (a) M∞=0.05, (b) M∞=0.3, (c) M∞=0.6, (d) M∞=0.9, and (e) M∞=1.2

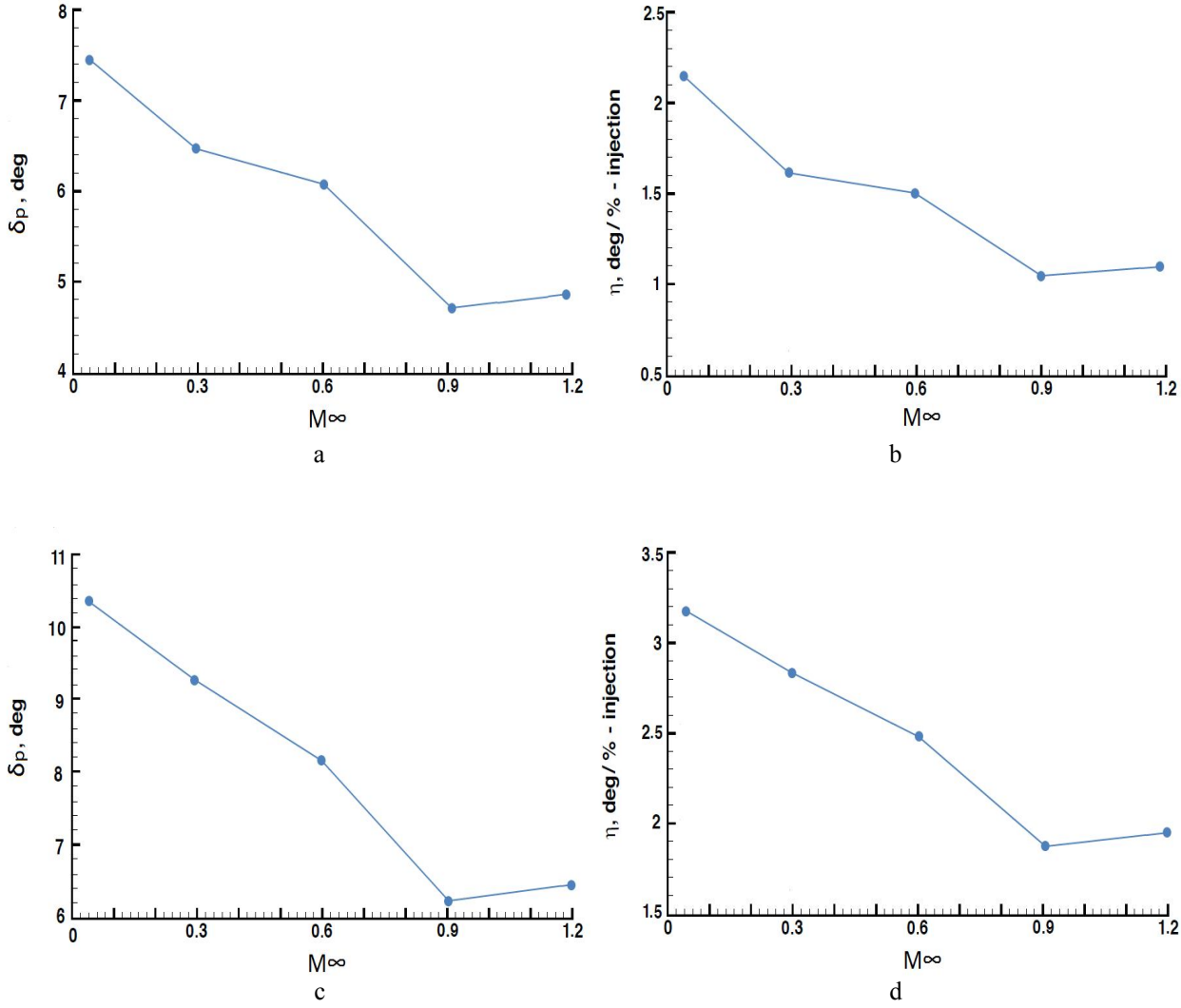

Fig. 7. Pitch thrust vector angle & thrust vectoring efficiency at NPR=4.6 and SPR=0.7 for (a)(b) normal to boundary injection angle and (c)(d) optimize injection angle

Conclusion

A computational investigation of the aerodynamic effects on fluidic thrust vectoring has been conducted. The effect of external freestream flow on pitch thrust vector angle on thrust vectoring efficiency was investigated. The performance of fluidic thrust vectoring was evaluated by studying thrust vector angle and thrust vectoring efficiency in nozzle exit. The effects of fluidic thrust vectoring parameters, such as NPR, SPR, and external freestream Mach number on FTV performance were studied. The data from the current computational investigation indicate that:

1) increasing the freestream Mach number, has negative impact on thrust vector angle and on thrust vectoring efficiency,

2) increasing freestream Mach number, decreases pitch thrust vector angle in all cases. Also decreases thrust vectoring efficiency in most cases,

3) the thrust vector angle in increasing freestream Mach number, which is achieved from 10.32° to 6.42° by the optimized fluidic injection angle, is decrease (10.5% to 37.7%); also from 7.57° to 4.33° by the normal to boundary fluidic injection angle is decrease (16.37% to 42.64%), and

4) the thrust vectoring efficiency is achieved from 3.099°/%- injection to 1.933°/%-injection by the optimized fluidic injection angle is decrease (10.5% to 37.6%). Also from 2.151°/%-injection to 1.107°/%-injection by the normal to boundary fluidic injection angle is decrease (24.73% to 48.53%).

References

1. Computational Study of an Axisymmetric Dual Throat Fluidic Thrust Vectoring Nozzle for a Supersonic Aircraft Application [Text] / K. A. Deere,

J. D. Flamm, B. L. Berrier [at all] // AIAA-2007-5085, July 2007. – 10 p.

2. Anderson, C. J. Investigation of Hybrid Fluidic [Text] / C. J. Anderson, V. J. Giuliano, D. J. Wing / Mechanical Thrust Vectoring for Fixed-Exit Exhaust Nozzles // AIAA 97-3148, July 1997. – 10 p.

3. Abeyounis, W. K. Static Internal Performance of an Overexpanded, Fixed-Geometry, Nonaxisymmetric Nozzle with Fluidic Pitch-Thrust-Vectoring Capability [Text] / W. K. Abeyounis, B. D. Bennett // NASA TP-3645, October 1997. – 18 p.

4. Fluidic Scale Model Multi-Plane Thrust Vector Control Test Results [Text] / C. Chiarelli, R. K. Johnsen, C. F. Shieh [at all] // AIAA Paper 93-2433, June 1993. – 7 p.

5. Giuliano, V. J. Static Investigation of a Fixed-Aperture Exhaust Nozzle Employing Fluidic Injection for Multiaxis Thrust Vector Control [Text] / V. J. Giuliano, D. J. Wing // AIAA Paper 97-3149, July 1997. – 21 p.

6. Wing, D. J. Fluidic Thrust Vectoring of an Axisymmetric Exhaust Nozzle at Static Conditions [Text] / D. J. Wing, V. J. Giuliano // ASME FEDSM97-3228, June 1997. – 12 p.

7. Deere, K. A. Computational Investigation of the Aerodynamic Effects on Fluidic Thrust Vectoring [Text] / K. A. Deere // AIAA-2000-3598, July 2000. – 100 p.

8. Waithe, K.A. An Experimental and Computational Investigation of Multiple Injection Ports in a Convergent-Divergent Nozzle for Fluidic Thrust Vectoring [Text] / K. A. Waithe // Master of Science Thesis, May 2001. – 10 p.

9. Deere, K. A. Summary of Fluidic Thrust Vectoring Research Conducted at NASA Langley Research Center [Text] / K. A. Deere // AIAA-2003-3800, June 2003. – 17 p.

10. Demonstration of Fluidic Throat Skewing for Thrust Vectoring in Structurally Fixed Nozzles [Text] / P. J. Yagle, D. N. Miller, K. B. Ginn [at all] // 2000-GT-0013, May 8-11, 2000. – 20 p.

11. Deere, K. A. PAB3D Simulations of a Nozzle with Fluidic Injection for Yaw-Thrust-Vector Control [Text] / K. A. Deere, D. J. Wing // AIAA Paper 98-3254, July 1998. – 28 p.

12. Miller, D. N. Fluidic Throat Skewing for Thrust Vectoring in Fixed Geometry Nozzles [Text] / D. N. Miller, P. J. Yagle, J. W. Hamstra // AIAA Paper 99-0365, January 1999. – 11 p.

13. Hunter, C. A. Computational Investigation of Fluidic Counterflow Thrust Vectoring [Text] / C. A. Hunter, K. A. Deere // AIAA Paper 99-2669, June 1999. – 21 p.

14. Flamm, J. D. Experimental Study of a Nozzle Using Fluidic Counterflow for Thrust Vectoring / J. D. Flamm // AIAA Paper 98-3255, July 1998. – 17 p.

15. Waithe, K. A. Experimental and Computational Investigation of Multiple Injection Ports in a Convergent-divergent Nozzle [Text] / K. A. Waithe, K. A. Deere // Fluidic Thrust Vectoring, the 21st / AIAA Applied Aerodynamics Conference // AIAA-2003-3802.

16. Deere, K. A. Propulsion simulations with the unstructured-grid CFD tool TetrUSS [Text] / K. A. Deere // AIAA 2002-2980. – 7 p.

17. Deere, K. A. Computational Investigation of the Aerodynamic Effects on Fluidic Thrust Vectoring [Text] / K. A. Deere // AIAA-2000-3598, July 2000. – 24 p.

18. Spalart, P. One-equation turbulence model for aerodynamic flows [Text] / P. Spalart, S. A. Allmaras // AIAA Paper 92-0439, January 1992. – 13 p.

19. Liou, M. S. Ten Years in the Making AUSA-family [Text] / M. S. Liou // AIAA Paper 2001-2521, Jun. 2001. – 12 p.

20. Liou, M. S. A Continuing Search for a Near-Perfect Numerical Flux Scheme [Text] / M. S. Liou // Technical Memorandum 106524, NASA, Mar. 1994. – 12 p.

21. Liou, M. S. A New Flux Splitting Scheme [Text] / M. S. Liou // Journal of Computational Physics. – 1993. – Vol. 107. – P. 33-39.

22. Muller, B. Runge-Kutta Finite Volume Simulation of Laminar Transonic Flow over a NACA0012 Airfoil, Using the Navier-Stokes Equation [Text] / B. Muller, A. Rizzi // FFA TN 1986-60. – 1989. – P. 40-48.

23. Van Leer, B. Towards the Ultimate Conservative Difference Scheme, Second-Order Sequel to Godunov's Method [Text] / Van Leer, B. // Journal of Computational Physics. – Jul. 1979. – Vol. 32, No. 1. – P. 101-136,

24. Hirsch, C. Numerical Computational of Internal and External Flows [Text] / John Wiley and Sons, Chichester. – 1988. – Vol. 2. – P. 123-132.

25. Van Albada, G. D. A Comparative Study of Computational Methods in Cosmic Gas Dynamics. [Text] / G. D. Van Albada, B. Van Leer, W. W. Roberts // Astronomy an Astrophysics. – 1982. – Vol. 108, No. 1. – P. 76-84.

Поступила в редакцию 1.06.2015, рассмотрена на редколлегии 19.06.2015

Reviewer: Ph.D, Assistant Prof. at Science and Research Branch, Mr. H. Mahdavy-Moghaddam, Islamic Azad University, Tehran, Iran.

ЧИСЛЕННОЕ ИССЛЕДОВАНИЕ АЭРОДИНАМИЧЕСКИХ МЕТОДОВ УПРАВЛЕНИЯ ВЕКТОРОМ ТЯГИ

Ф. Форгани, М. Таеби-Рани, А. Асадоллахи-Гохие

Представлено выполненное с помощью вычислительных методов исследование аэродинамических методов управления вектором тяги. Моделирование двумерного сужающегося-расширяющегося (2DCD) сопла с управлением направлением вектора тяги методом инжектирования потока выполнено с помощью CFD с использованием модели турбулентности Спаларта-Аллмараса (S-A). Рассмотрены условия отсутствия движения (M=0.05), а также полета в диапазоне чисел Маха от 0.3 до 1.2 при значениях отношения давлений в сопле 4.6 и отношении полных давлений в наружном и внутреннем потоках 0.7. Аэродинамические потери углового отклонения вектора тяги составили от 3.9 градусов при M=1.2 до 1.08 градусов при M=0.3 (по сравнению с положением вектора тяги при отсутствии движения). Полученные результаты показали, что набегающий поток уменьшает отклонение вектора тяги по сравнению с условиями, в которых находится неподвижный двигатель.

Ключевые слова: управление вектором тяги, влияние скорости внешнего потока.

ЧИСЕЛЬНЕ ДОСЛІДЖЕННЯ АЕРОДИНАМІЧНИХ МЕТОДІВ КЕРУВННЯ ВЕКТОРОМ ТЯГИ

Ф. Форгані, М. Таебі-Рані, А. Асадоллахі-Гохіе

Представлено виконане за допомогою обчислювальних методів дослідження аеродинамічних методів керування вектором тяги. Моделювання двомірного звужувано-розширюючогося сопла з керуванням напрямком вектора тяги методом інжектування потоку виконано за допомогою CFD із використанням моделі турбулентності Спаларта-Аллмараса (S-A). Розглянуто умови відсутності руху (M=0.05), а також польоту в діапазоні чисел Маха від 0.3 до 1.2 при значеннях відношення тисків у соплі 4.6 і відношенні повних тисків у внутрішньому та зовнішньому потоках 0.7. Аеродинамічні втрати кутового відхилення вектора тяги склали від 3.9 градусів при M=1.2 до 1.08 градусів при M=0.3 (порівняно з положенням вектора тяги за відсутністю руху). Отримані результати показали, що набіжний потік зменшує відхилення вектора тяги у порівнянні з умовами, в яких знаходиться нерухомий двигун.

Ключові слова: керування вектором тяги, вплив швидкості зовнішнього потоку.

Forghany Farzad – Ph.D, Candidate of Mechanical and Aerospace Engineering Department, Science and Research Branch, Islamic Azad University, Tehran, Iran, e-mail: farzad_forghany@yahoo.com.

Taiebi-Rahni Mohammad – Professor of Aerospace Engineering Department, Sharif University of Technology, Tehran, Iran, e-mail: taeibi@sharif.edu, (Corresponding Author).

Asdollahi-Ghohieh Abdollah – Assistant Professor of Aerospace Engineering Department, Civil Aviation Technology College, Tehran, Iran, e-mail: ghohieh@yahoo.com.